Particle Accelerators, 1987, Vol. 22, pp. 81–99
Photocopying permitted by license only

Printed in the United States of America

BEAM LOADING IN PLASMA ACCELERATORS

T. KATSOULEAS, S. WILKS, P. CHEN,† J. M. DAWSON and J. J. SU
Department of Physics, University of California, Los Angeles, CA 90024

(Received April 21, 1986; in final form September 25, 1986)

We address the issue of beam loading in the plasma beat-wave and plasma wake-field accelerator schemes. We find the total number of particles which can be accelerated and the resulting efficiency subject to constraints on emittance growth and energy spread. The analytic predictions are compared to 1-D computer simulations.

1. INTRODUCTION

Acceleration of particles in high-phase-velocity plasma waves is attractive because of the extremely high accelerating gradients that can be obtained.[1–3] However, a high gradient is only one important benchmark for an accelerator. It is also important to know how many particles can be accelerated (i.e., luminosity), what will be the beam quality (i.e., emittance), and what will be the overall efficiency of the device. In this paper, we address these issues for plasma-wave accelerators. The results apply to both the beat-wave[2,4] and wake-field[3,5,6] accelerator schemes.

Previous work by R. Ruth et al.[5] has addressed emittance matching in plasma wake fields driven by unshaped electron bunches. S. Van der Meer[7] has considered specialized shaping of an accelerated beam to reduce its energy spread. Here we consider simultaneously the constraints on emittance and energy spread. These lead to quantitative estimates of the maximum number of particles that can be accelerated in plasma waves and the resulting efficiency. We augment the analysis with self-consistent particle-in-cell computer simulations.

In order to find the maximum number of particles that can be accelerated by a plasma wave, we first review the wake field generated by a relativistic charged-particle bunch of arbitrary shape (Section 2). The beam-loading problem can then be analyzed by applying linear superposition of the bunch wake field and the accelerating plasma-wave field. This is done for a one-dimensional approximation in Section 3 and for three dimensions in Section 4.

2. THE WAKE-FIELD RESPONSE IN A 3-D COLD PLASMA

In this section, we find the electric field response of a cold plasma to a bunch of arbitrary charge moving at approximately c. This can be found from the Green's

† University of California, Los Angeles, and Stanford Linear Accelerator Center, Stanford, CA 94305.

function response to a single test charge. Such a wake (or Green's) function has been found previously using potentials (ϕ, $\mathbf{A}$).[3,8] The derivation is simplified by solving directly for the fields,[9] as in the following.

Consider a charge q of velocity $\mathbf{V}_b$ moving through a plasma. It represents an external charge density

$$\rho_0 = q\delta(\mathbf{X} - \mathbf{V}_b t) = q\delta(\mathbf{r})\delta(z - V_b t), \tag{1}$$

where the z axis is chosen to correspond to the direction of $\mathbf{V}_b$, $\mathbf{r}$ is the radial polar coordinate, and $\delta(\mathbf{r}) = 1/(2\pi r)\delta(r)$. The response of the cold plasma can be found from the linearized equations of motion, continuity, and Maxwell's equations:

$$\frac{d\mathbf{V}}{dt} = -e\mathbf{E}/m, \tag{2}$$

$$\frac{\partial n_1}{\partial t} + n_0 \nabla \cdot \mathbf{V} = 0, \tag{3}$$

$$\nabla \cdot \mathbf{E} = -4\pi e n_1 + 4\pi\rho_0 \tag{4}$$

$$\nabla \times \mathbf{E} = -\frac{1}{c}\frac{\partial \mathbf{B}}{\partial t}, \tag{5}$$

$$\nabla \times \mathbf{B} = (4\pi/c)\mathbf{j} + \frac{1}{c}\frac{\partial \mathbf{E}}{\partial t}, \tag{6}$$

where n_0, n_1 are the background and perturbed plasma density; $\mathbf{V}$ and $\mathbf{E}$ are the perturbed velocity and electric field of the plasma.

Taking the first derivative of Eq. (3) and substituting from Eq. (2) gives

$$\frac{\partial^2 n_1}{\partial t^2} + n_0 \nabla \cdot (-e\mathbf{E}/m) = 0.$$

Substituting for $\nabla \cdot \mathbf{E}$ from Poisson's equation [Eq. (4)] gives the wave equation for the plasma density response:

$$\frac{\partial^2 n}{\partial t^2} + \omega_p^2 n_1 = (n_0 e/m)(4\pi\rho_0) = \omega_p^2 (q/e)\delta(\mathbf{r})\delta(t - z/V_b)/V_b, \tag{7}$$

where $\omega_p^2 = 4\pi n_0 e^2/m$, and where we have used Eq. (1) and the fact that $\delta(z - V_b t) = \delta(t - z/V_b)/V_b$. The solution to Eq. (7) is just the Green's function for a harmonic oscillator namely,

$$n_1 = [\omega_p q\delta(\mathbf{r})/V_b e] \sin \omega_p (t - z/V_b)\theta(t - z/V_b), \tag{8}$$

where θ is the step function which is 1 or 0 for positive or negative values of its argument.

Using this expression for the density in Eqs. (5) and (6), we can obtain the fields. Taking the curl of Eq. (5) and substituting the time derivative of Eq. (6) in

the usual way gives the wave equation for $\mathbf{E}$:

$$\left(\frac{\partial^2}{\partial t^2} - c^2\nabla^2\right)\mathbf{E} = -4\pi\frac{\partial \mathbf{j}}{\partial t} - c^2\nabla(\nabla\cdot\mathbf{E}). \tag{9}$$

Now,

$$\frac{\partial \mathbf{j}}{\partial t} = -n_0 e\frac{\partial \mathbf{V}}{\partial t} = n_0 e^2\mathbf{E}/m$$

[from Eq. (2)], and $\nabla\cdot\mathbf{E}$ is given by Eqs. (4) and (8). Thus, Eq. (9) becomes

$$(\nabla_\perp^2 - k_p^2)\mathbf{E} = (-4\pi\omega_p q/c)\nabla[\delta(\mathbf{r})\theta(t - z/c)\sin\omega_p(t - z/c)],$$

where we have separated ∇^2 into $\nabla_\perp^2 + \partial^2/\partial z^2$ and assumed that the z, t dependence of the wake fields is a function only of the combination $(z - V_b t) \cong (z - ct)$ [i.e., $\partial^2/\partial t^2 = c^2(\partial^2/\partial z^2)$]; $k_p^2 \equiv \omega_p^2/c^2$.

For the longitudinal wake field E_z, this gives

$$(\nabla_\perp^2 - k_p^2)E_z = 4\pi q k_p^2\delta(\mathbf{r})\theta(t - z/c)\cos\omega_p(t - z/c). \tag{10}$$

The radial dependence of E_z is simply the Green's function response to the Kelvin–Helmholtz equation; that is,

$$E_z = -2qk_p^2 K_0(k_p r)\theta(t - z/c)\cos\omega_p(t - z/c), \tag{11}$$

where K_0 is the zeroth-order modified Bessel function of the second kind.

The transverse wake function is easily obtained from Eq. (11) and the Panofsky–Wenzel theorem[10] for wake fields which are a function of $z - ct$. The theorem follows directly from the θ component of Eq. (5) and gives

$$\frac{\partial W_\parallel}{\partial r} = \frac{\partial W_\perp}{\partial z},$$

where

$$W_{\parallel,\perp} = \left(\mathbf{E} + \frac{\mathbf{V}\times\mathbf{B}}{c}\right)_{z,r}$$

are the longitudinal and transverse wake functions ($\mathbf{V} = c\hat{z}$). Since $W_\parallel$ is E_z and

$$\frac{d}{dx}K_0(x) = -K_1(x),$$

we have

$$W_\perp = (E_r - B_\theta) = \int dz\frac{\partial W_\parallel}{\partial r} = -2qk_p^2 K_1(k_p r)\theta(t - z/c)\sin\omega_p(t - z/c). \tag{12}$$

Equations (11) and (12) describe the wake fields produced behind a single charge. The wake fields produced by an arbitrary beam of relativistic particles of charge density $\rho_b(r, \theta, z - ct)$ can be found by integrating over Eq. (12) as follows:

$$E_z(r, \theta, \zeta) = (-2k_p^2)\int_{+\infty}^{\zeta} d\zeta'\int_0^\infty r'\,dr'\int_0^{2\pi} d\theta'\rho_b(r', \theta', \zeta') \tag{13}$$
$$\times K_0(k_p|\mathbf{r} - \mathbf{r}'|)\cos k_p(\zeta - \zeta'),$$

where $\zeta \equiv z - ct$ and the perpendicular distance $|\mathbf{r} - \mathbf{r}'|$ is given by $[r^2 + r'^2 - 2rr' \cos(\theta - \theta')]^{1/2}$.

If the charge density ρ_b is separable [i.e., $\rho_b = \rho_{\parallel}(\zeta) \cdot \rho_{\perp}(r, \theta)$], then the response can be expressed as

$$W_{\parallel} = E_z(r, \zeta) = Z'(\zeta)R(r), \tag{14a}$$

where

$$Z'(\zeta) = -4\pi \int_{\infty}^{\zeta} d\zeta' \rho_{\parallel}(\zeta') \cos k_p(\zeta - \zeta'),$$

$$R(r) = \frac{k_p^2}{2\pi} \int_0^{2\pi} d\theta \int_0^{\infty} r'\, dr' \rho_{\perp}(r', \theta) K_0(k_p |\mathbf{r} - \mathbf{r}'|).$$

Similarly, the transverse wake fields are

$$W_{\perp} = Z(\zeta)R'(r), \tag{14b}$$

where

$$Z' \equiv \frac{\partial Z}{\partial \zeta} \quad \text{and} \quad R' \equiv \frac{\partial R}{\partial r}.$$

3. WIDE, UNIFORM BEAMS (1-D ANALYSIS)

When the particle beam and the accelerating wave have nearly uniform transverse profiles and are much larger than c/ω_p, the beam-loading problem is approximately one-dimensional. In this section, we examine this simplified case analytically and with 1-D computer simulations.

The 1-D Green's function wake field produced by a test charge is easily obtained from Eq. (10) by replacing $\delta(\mathbf{r}_{\perp})$ by 1 and $\nabla_{\perp}^2$ by 0.[5] Then, in one dimension for an infinitesimally thin sheet of charge per unit area q/A,

$$E_z = (-4\pi q/A)\theta(t - z/c) \cos \omega_p(t - z/c). \tag{15}$$

For a volume charge density $\rho_b(z)$,

$$E_z \equiv Z'(\zeta) = -4\pi \int_{\infty}^{\zeta} d\zeta' \rho_b(\zeta') \cos k_p(\zeta - \zeta'). \tag{16}$$

Note that one would obtain the same result from Eq. (14) with $\rho_{\perp} = 1$.

3.1. Short, Unshaped Beams

In a cold plasma, the wake function, Eq. (15), is a simple sinusoid, just as is the accelerating wave field,[1,11] (whether created by beat wave, wake field, or other means):

$$E_z^{\text{wave}} = E_0 \cos(\omega_p t - k_p z + \phi) = (-4\pi e n_1/k_p) \cos(\omega_p t - k_p z + \phi), \tag{17}$$

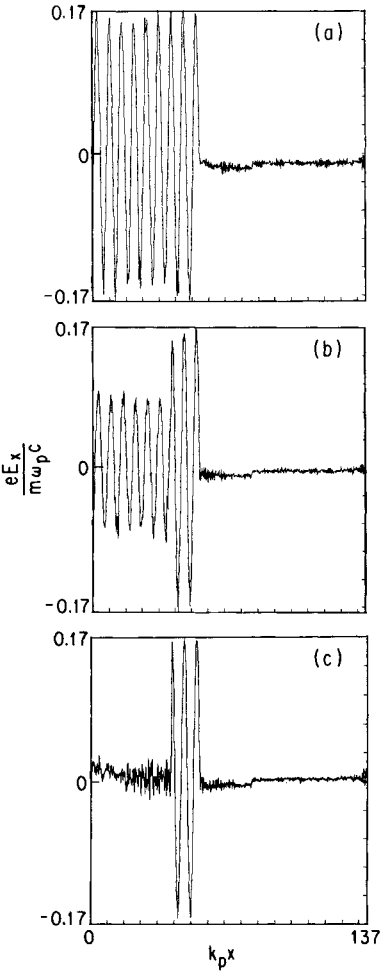

FIGURE 1 Total electric field in a 1-D simulation loaded with short bunches of (a) 0, (b) $0.5N_0$, and (c) N_0 (positively charged) electrons on the third peak of an accelerating wave. Simulation consisted of 14,000 partricles on 19024 grids; system length = $170c/\omega_p$, particle size = $0.11c/\omega_P \cong$ bunch width, wave amplitude $n_1 \cong 0.16n_0$ (produced by wake-field mechanism), time step = $0.04\omega_p^{-1}$, $\omega_p t = 40$, $\gamma^{\text{beam}} = \gamma^{\text{wave}} = 60$.

where n_1 is the perturbed plasma density associated with the wave ($< n_0$) and ϕ is a constant phase factor. Thus, one could exactly cancel the accelerating wave field by placing a short ($\ll c/\omega_p$) beam of electrons at a minimum of the accelerating wave ($\phi = 0$, see Fig. 1). Comparison of Eqs. (17) and (15) shows that behind the beam, the total field ($E^{\text{wave}} + E^{\text{beam}}$) equals zero if $q = -Ne$ and the number of electrons N is given by

$$N_0 = \frac{E_0}{4\pi e} \cdot A \cong \frac{n_1}{k_p} A \cong 5 \times 10^5 \left(\frac{n_1}{n_0}\right) \sqrt{n_0}\, A, \tag{19}$$

where n_0 is in cm^{-3} and A is in cm^2 in the last expression. For a wave of 1-cm^2

cross section in a plasma of density $10^{16}\,\mathrm{cm}^{-3}$ and $n_1/n_0 \cong 0.2$, N_0 is approximately 10^{13}.

Figure 1 illustrates the total electric field in 1-D electrostatic particle-in-cell computer simulations. Typically, in the simulations, 10^4 particles are followed on a simulation grid $100\,c/\omega_p$ long consisting of 500 cells. The charge density represented by these particles is evaluated in each cell and used to find the electric field (from Poisson's equation) at each particle. The Lorentz force is then used to leapfrog the particles through one time step (typically $0.1\,\omega_p^{-1}$). The new charge density can be computed, and the process repeated. Short beams of 0, 0.5 N_0, and N_0 (positively charged) electrons were placed at the third peak of an accelerating wave. As expected, the electric field is nearly perfectly canceled in the last case. Simulation parameters are given in the figure caption.

Equation (19) represents the maximum number of electrons that can be accelerated in an ultrashort, unshaped bunch. Since all of the wave energy is absorbed, this idealized case corresponds to 100% beam-loading efficiency. We note that such an idealized case is not possible (even theoretically) in conventional accelerating cavities. In conventional structures, the wake function of a single charge (or a short bunch) is nonsinusoidal[12] because a structure typically has many modes which can be excited by a short bunch. So a short bunch cannot exactly cancel the accelerating waveform, which is generally sinusoidal (although the higher modes are less excited by long bunches). This disadvantage is compensated by the fact that the energy not removed from a high-Q cavity is not wasted but is stored while the accelerating wave is replenished for the next bunch. In a plasma, recovering unused energy is more difficult, because any remaining wave energy may couple to competing plasma instabilities before it can be replenished.

Unfortunately, in our idealized beam-loading model, 100% efficiency is achieved only at the expense of 100% spread in the energy gain of the beam. This is because an electron at the front of this infinitesimally short beam feels the full accelerating field E^{wave}, while the last electron feels the superposed field $E^{\mathrm{wave}} + E^{\mathrm{beam}} = 0$ (see Fig. 1). Since the reduction in accelerating field for the last particle is linear in the number of particles loaded, N, the fractional energy spread will be

$$\frac{\Delta\gamma_{\max} - \Delta\gamma_{\min}}{\Delta\gamma_{\max}} = \frac{E_i - E_f}{E_i} = \frac{N}{N_0}, \tag{20}$$

where $E_{i,f}$ are the field amplitudes in front of and behind the accelerated bunch, and $\Delta\gamma_{\max,\min}$ refer to the maximum and minimum energy gain by a particle in the bunch. On the other hand, the fraction of wave energy absorbed by the particles is $1 - E_f^2/E_i^2$. Since $E_f = E_i(1 - N/N_0)$, the beam-loading efficiency is

$$\eta_b = \frac{N}{N_0}\left(2 - \frac{N}{N_0}\right). \tag{21}$$

Equations (20) and (21) illustrate the tradeoff between energy spread and efficiency for short, unshaped beams. The beam-loading efficiency measured in

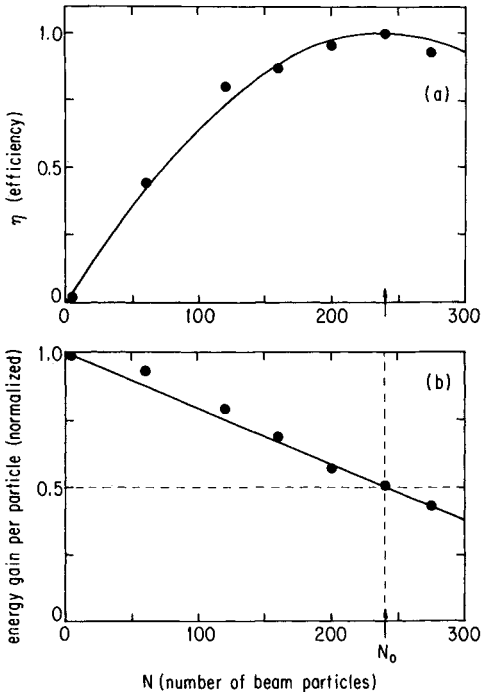

FIGURE 2 (a) Beam-loading efficiency in 1-D simulations vs number of particles in beam [solid curve is from Eq. (21)]; and (b) average energy gain per particle vs number in beam.

the 1-D computer simulations vs particle number is plotted in Fig. 2 and compared with Eq. (21).

3.2. Tailoring the Beam Distribution

In order to reduce the energy spread of the beam without lowering the beam-loading efficiency, two methods of tailoring the beam distribution have been suggested. The first idea[13] is to divide the desired number of particles, N, into m bunches, positioned, as in Fig. 3, such that the last bunch is at a phase corresponding to a peak of the accelerating wave and each preceding bunch is advanced in phase by one wavelength plus $\delta\phi_m$, so that it feels the same value of

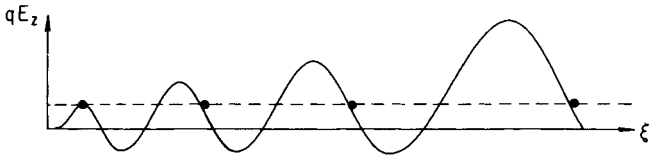

FIGURE 3 Scheme to reduce energy spread by varying the phases of several bunches; each feels the same accelerating field.

E_z. Since there are only N/m particles in each bunch, the fractional energy spread in the wide beam might be reduced by the factor m.

A variation of this scheme appears to be well-suited to the beat-wave accelerator. Since the wave amplitude increases downstream in the growth portion of the beat-wave accelerator, it is possible to place each bunch at the same phase (i.e., $\delta\phi_m = 0$). By choosing the proper number of particles in each bunch, one can compensate for growth of the wave so that each bunch is accelerated at the same rate.

A more effective way of reducing the energy spread which allows for the finite length of realistic beams has been suggested by S. Van der Meer.[7] Here, the accelerated beam is ramped down in density in much the same way that the driving beam of the plasma wake-field accelerator is ramped up.[6] The appropriate shape of the beam, $\rho_b(\zeta)$, can be found from Eqs. (16) and (17), and from the requirement that the superposition of the wake and wave fields be constant inside the beam. That is,

$$E_a = E_0 \cos k_p\zeta - 4\pi \int_{\zeta_0}^{\zeta} d\zeta' \rho(\zeta') \cos k_p(\zeta - \zeta'),$$

where E_a is the constant accelerating field and ζ_0 is the location of the head of the bunch. Assuming that the bunch density $\rho_b(\zeta)$ is of the form $a\zeta + b$, beginning at $\zeta = \zeta_0$ ahead of the wave minimum, and solving for a and b gives

$$\rho_b(\zeta) = -\frac{k_p E_0}{4\pi}[(k_p \cos k_p\zeta_0)\zeta + (\sin k_p\zeta_0 - k_p\zeta_0 \cos k_p\zeta_0)] \tag{22}$$

and $-k_p E_0/4\pi e = n_1$, the density perturbation associated with the wave.

This corresponds to a triangular bunch shape with the peak density at the head of the bunch, as in Fig. 4a (the back of the bunch could be truncated at any point to give a trapezoidal shape, as in Fig. 4c). The maximum allowable bunch length is determined by the condition that ρ_b does not change sign. The corresponding peak bunch density, maximum bunch length, accelerating field, and number of particles are

$$\rho_b(\zeta_0) = \rho_b^{\max} = -en_1 \sin k_p\zeta_0, \tag{22a}$$

$$\ell_{\max} = (\tan k_p\zeta_0)k_p^{-1}, \tag{22b}$$

$$E_a = E_0 \cos k_p\zeta_0, \tag{22c}$$

$$N = N_0 \frac{\sin^2 k_p\zeta_0}{2 \cos k_p\zeta_0}, \tag{22d}$$

where N_0 is $n_1 A/k_p$, as defined in Eq. (19), with A the cross-sectional area of the waves and beams (assumed much wider than c/ω_p). The beam-loading efficiency is given by $1 - E_a^2/(E^{\text{wave}})^2 = 1 - \cos^2 k_p\zeta_0$, or

$$\eta_b = \sin^2 k_p\zeta_0 \tag{22e}$$

for the specially shaped beams.

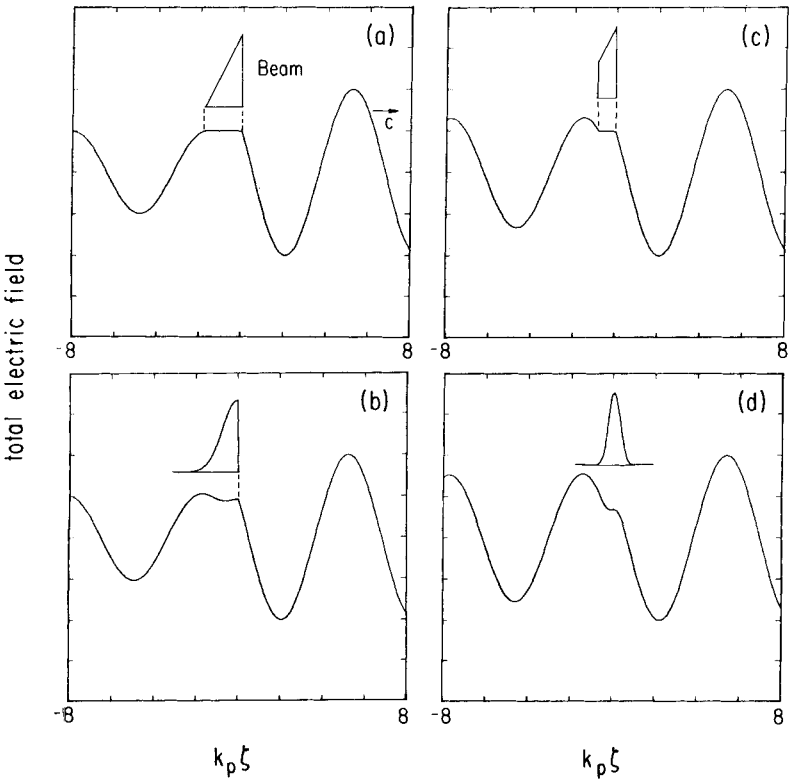

FIGURE 4 Total electric field for various beam shapes: (a) triangle [Eq. (22), $N = 3N_0/4$, $k_p\zeta_0 = \pi/3$), (b) half-Gaussian of same number of particles, (c) truncated triangle ($N = 9N_0/16$), and (d) Gaussian of same number as (c).

Although such shaped bunches suffer no energy spread, Eqs. (22) show the tradeoff between accelerating gradient on the one hand, Eq. (22c), and efficiency (22e) or total particle number on the other, Eq. (22d). For example, if one places the front of a triangular bunch ahead of the wave-field minimum by an amount $\zeta_0 = \pi/3k_p$, with $N = 3N_0/4$ particles over a length $\sqrt{3}/k_p$, then the predicted gradient is 50% of the peak accelerating wave amplitude and the beam-loading efficiency is 75%, without energy spread.

In Fig. 5, the results of a 1-D simulation corresponding to this example are shown.

3.3. Gaussian Bunches

Since shaping of bunches on a scale as small as k_p^{-1} may prove difficult, we consider the consequences of Gaussian bunch shapes. We compare them to a triangular bunch truncated at length $\ell = \ell_{\max}/2$ [thus containing three fourths of the number of particles given in Eq. (22d)]. The Gaussian bunch density is of the

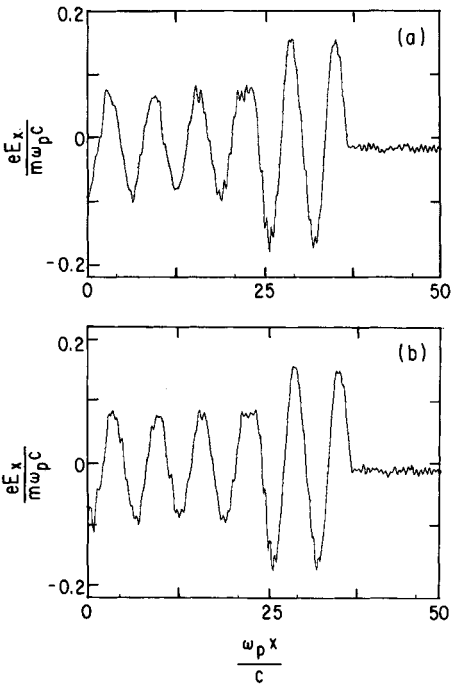

FIGURE 5 One-dimensional simulations of (a) triangular beam loading [Eq. (22), $N = 3N_0/4$, $k_p\ell = \sqrt{3}$] and (b) same number in a Gaussian of width $k_p\sigma = \sqrt{3}/2$ located at the weighted center of the triangle ($\omega_p r = 20$).

form

$$\rho_b(\zeta) = (-en_1 \sin k_p\zeta_0) \exp\left[-(\zeta - \zeta_0 + \ell/2)^2/2\sigma^2\right],$$

where σ is $3\ell/8\sqrt{2\pi}$, so that the total number is that of the half triangle. The resulting total field is shown in Fig. 4d (for $k_p\zeta_0 = \pi/3$). For particles within 1σ of the center, the accelerating field is approximately one third of the wave amplitude and varies by $\lesssim \pm 10\%$. For the same number of particles in an ultrashort bunch (at $\zeta_0 = 0$), Eq. (20) predicts an energy spread of 56%. Thus, a well-placed Gaussian may suffer less energy spread than an ultrashort bunch, but more than the ideally shaped bunch. One-dimensional simulations of the fields and particle energies for Gaussian bunches are shown in Figs. 5 and 6.

3.4. Phase Slippage

Thus far, we have neglected the phase slippage of the accelerated bunch in the plasma wave. Since the energy gain of particles in the wave frame is analogous to the energy gain of a marble rolling down a potential hill, energy gain then necessarily entails phase slippage. For either the beat-wave or wake-field schemes, the total phase slippage can be expressed in terms of the energy gain $\Delta\gamma$ as roughly

$$\Delta\phi \cong \frac{\Delta\gamma}{2\gamma_\phi^2}\frac{n_0}{n_1}, \tag{23}$$

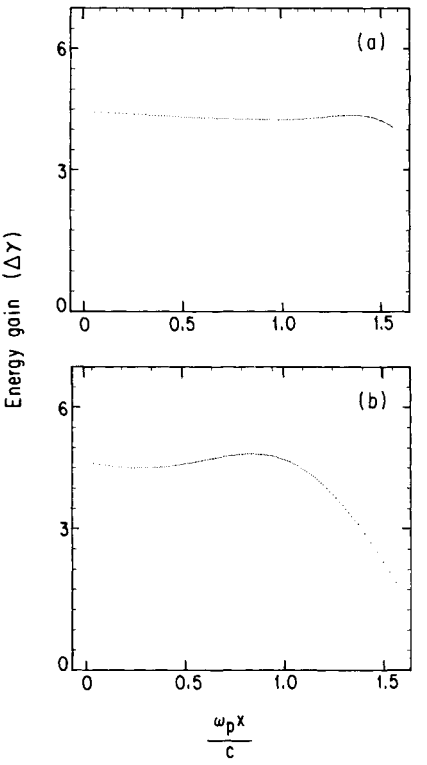

FIGURE 6 Energy gain of beams in simulation of Fig. 5 ($\omega_p t = 40$).

where γ_ϕ is the Lorentz factor associated with the wave velocity and $\Delta\gamma \gg \gamma_\phi \gg 1$. For the wake-field accelerator, $\gamma_\phi = \gamma_b$ of the driving electron beam; for the beat-wave accelerator, $\gamma_\phi \cong \omega_0/\omega_p$, where ω_0 is the laser frequency. For the wake-field accelerator, the phase slippage can be kept quite small by using very relativistic driving beams.[5] Moreover, it has been shown in the last of Refs. 6 that phase slippage can be avoided altogether by tailoring the plasma density appropriately. For the beat-wave accelerator, it is more difficult to avoid phase slippage, but this may be accomplished by the Surfatron phase-locking scheme, which employs a transverse magnetic field (see the second of Refs. 4).

To eliminate energy spread, Eqs. (22) specify the beam shape as a function of the beam placement (ζ_0). Since phase slippage alters this placement, it makes the accelerating field nonuniform and hence causes energy spread. When the bunch slips in phase from its ideal location by an amount $\Delta\phi$, the total electric field within the bunch becomes

$$\begin{aligned} E &= E_{\text{wave}} + E_{\text{beam}} \\ &= E_0 \cos k_p\zeta + E_0[\cos(k_p\zeta_0 + \Delta\phi) - \cos(k_p\zeta + \Delta\phi)]. \end{aligned}$$

When $\Delta\phi = 0$, $E = E_0 \cos k_p\zeta_0 = E_a$, as we expect. For $\Delta\phi \ll 1$, the energy

spread induced by the electric field variation over the length of the bunch is approximately

$$\frac{\delta E}{E} \cong \frac{1}{2}\frac{\Delta\phi}{\cos k_p\zeta_0}\,\delta(\sin k_p\zeta),$$

where the factor of $\frac{1}{2}$ arises because the average phase of the accelerated particles is one half their maximum phase slippage, and where $\delta(\sin k_p\zeta)$ represents the maximum variation of $\sin k_p\zeta$ over the length of the bunch (i.e., as ζ varies from ζ_0 to $\zeta_0 - \ell$). For bunch lengths $k_p\ell \ll 1$ *or* $k_p\ell \cong k_p\ell_{\max} = \tan k_p\zeta_0$ (but $k_p\ell$ not necessarily small), the above expression is approximately

$$\frac{\delta E}{E} = \tfrac{1}{2}\Delta\phi \cdot k_p\ell. \tag{24}$$

For our previous example, $k_p\ell_{\max}$ was equal to 2 so that a 0.1-radian phase error gives a maximum 10% energy spread. Smaller energy spread can be obtained by truncating the bunches.

Energy spread may also be caused by bunch placement errors. In that case, the energy spread expression analogous to Eq. (24) is $\delta E/E \cong \Delta\phi k_p\ell$, where $\Delta\phi$ is the phase of the front of the bunch relative to its ideal phase $k_p\zeta_0$.

4. TRANSVERSE BEAM-LOADING CONSIDERATIONS

The beam loading described in the previous section is valid when the beams and the accelerating waves have the same transverse profile and are wide compared to c/ω_p. In this section, we consider beams of arbitrary width. We find the limits on beam radius, beam number, and efficiency imposed by emittance and energy spread constraints.

We begin by considering the wake-field response to uniform beams cut off at arbitrary radius a: $\rho_b(r, \theta, \zeta) \equiv \rho_b(\zeta)\theta(a - r)$. (For narrow beams, the conclusions we draw will be largely independent of the exact form of the radial profile.) From Eq. (14), the wake field is separable into longitudinal and transverse factors: $E_z = Z'(\zeta)R(r)$. To evaluate $R(r)$, we use the identity[14]

$$K_0[k_p(r^2 + r'^2 - 2rr'\cos\theta)^{1/2}] = I_0(k_pr_<)K_0(k_pr_>) + 2\sum_{m=1}^{\infty}\cos m\theta I_m(k_pr_<)K_m(k_pr_>),$$

where $r_{>,<}$ denote the larger or smaller of r and r'. Noting that the integral of the last term over θ vanishes, we obtain[15]

$$R(r) = \begin{cases} 1 - k_paK_1(k_pa)I_0(k_pr) & (r < a), \\ k_paI_1(k_pa)K_0(k_pr) & (r > a). \end{cases} \tag{25}$$

This radial function is plotted in Fig. 7 (normalized to 1 at $r = 0$) for values of k_pa from 0.001 to 1. Although the beam radii differ by orders of magnitude, their radial wake profiles do not. Physically, this means that even very narrow beams can absorb plasma wave energy out to a skin depth c/ω_p.

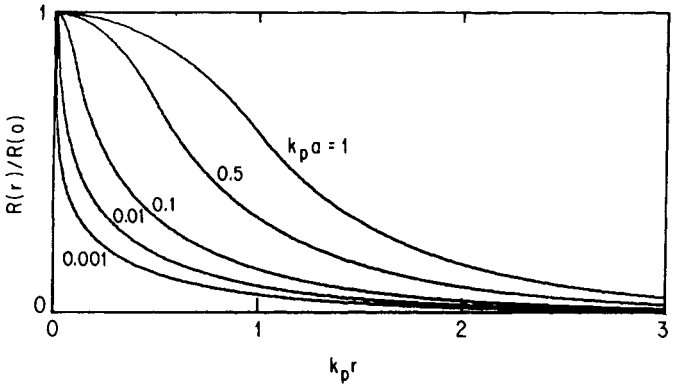

FIGURE 7 Radial profiles of longitudinal wake fields for uniform beams of various radii.

For wide beams ($k_p a \gg 1$), Eq. (25) gives $R(r) \cong 1$ inside the beam and $R(r) \cong 0$ outside. The radial factor on axis is $R_a(0) = 1 - k_p a K_1(k_p a)$, which can be much less than unity (see Fig. 8) for narrow beams. To produce the same size wake field on axis as does a wide beam, a narrow beam must have a beam density which is $1/R_a(0)$ times higher. Thus, the 3-D beam shaping counterpart to Eq. (22) is

$$\rho_b(\zeta) = \frac{-k_p E_0}{4\pi R_a(0)} [(k_p \cos k_p \zeta_0)\zeta + (\sin k_p \zeta_0 - k_p \zeta_0 \cos k_p \zeta_0)], \tag{22'}$$

where E_0 is the plasma wave amplitude on axis. The corresponding number of particles in the accelerated beam, given by Eq. (22d) for the ideal triangular beams and Eq. (19) for short beams, is

$$N = N_0 \frac{\sin^2 k_p \zeta_0}{2 \cos k_p \zeta_0}, \tag{22d}$$

where

$$N_0 = (E_0/4\pi e) A_{\text{eff}} \tag{19'}$$

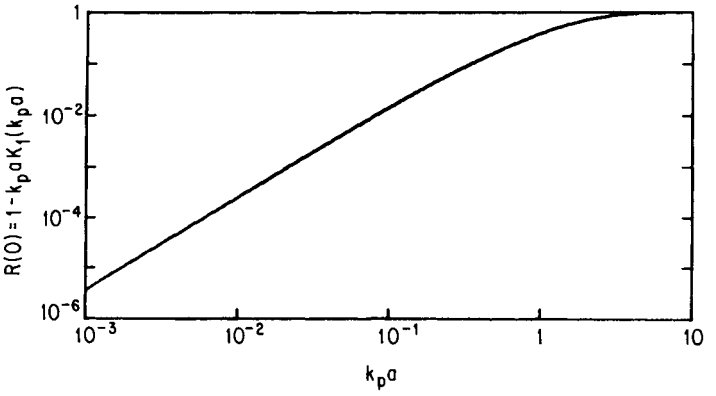

FIGURE 8 The factor $R_a(0)$ in Eqs. (25), (22') and (19').

and A_{eff} is the effective area of the beam defined by

$$A_{\text{eff}} = \frac{\pi a^2}{1 - k_p a K_1(k_p a)}. \tag{19a'}$$

For $k_p a \ll 1$, $A_{\text{eff}}\pi = \pi a^2 = A$, and for $k_p a \ll 1$, $A_{\text{eff}} \cong (\pi c^2/\omega_p^2)[-2/(0.577 + \ln k_p a/2)] = O(c^2/\omega_p^2)$. For a wide range of $k_p a \ll 1$, the effective area remains of order c^2/ω_p^2 ($A_{\text{eff}} = 0.6$ to 2 times c^2/ω_p^2 for $k_p a = 10^{-4}$ to 10^{-1}). Thus, in the small-beam limit, the exact form of the radial beam profile is unimportant. For such narrow beams, it is the beam number (Eq. 19′) rather than the beam density that is relevant. In fact, the beam density may become even larger than the plasma density without violating the assumptions of our linear analysis (as long as the resulting wake fields do not approach the wave-breaking amplitude $E = mc\omega_p/e$). A qualitative statement of these effects was given previously by R. Evans.[16]

4.1. Emittance

Constraints on emittance limit the allowable radius of the accelerated beam. The transverse emittance of the beam is proportional to the area in transverse phase space, $\varepsilon \equiv rV_r/c$. If the beam is subject to a transverse focusing force,[5,11] it will undergo betatron oscillations of wavelength $2\pi\beta$. The beam radius is related to the emittance and the β function by

$$a^2 = \varepsilon\beta.$$

To estimate β, consider a plasma wave of parabolic profile, $W_{\parallel} = E_z = E_0 (1 - r^2/w^2) \cos k_p \zeta (r < w)$. Then from the Panofsky–Wenzel theorem,

$$W_{\perp} = \int \frac{dW_{\parallel}}{\partial r}\, dr \cong E_r = (-2r/k_p w^2) E_0 \sin k_p \zeta,$$

and ζ is the position of the particle relative to the point of maximum acceleration. This gives a betatron function for a particle of energy γ

$$\beta \cong w(\gamma mc\omega_p/2eE_0 \sin k_p \zeta)^{1/2}, \tag{26}$$

Thus, the beam radius is given by

$$a \leq (w\varepsilon)^{1/2}(\gamma mc\omega_p/2eE_0 \sin k_p \zeta_0)^{1/4}. \tag{27}$$

To keep the emittance small, Eq. (27) suggests the use of either wide waves or very narrow beams. The width of the wave is governed by the driving source. For laser–driven waves, self-focusing may cause the laser to contract asymptotically to a beam waist of order c/ω_p.[17] For electron beam–driven waves, the waves may need to be kept at least this wide to avoid radiative losses due to betatron motion of the driving beam.[18]

As an example, consider the (nonoptimized) beam requirements suggested by B. Richter[19] for a future 5-TeV collider. To achieve a luminosity of $10^{34}\ \text{cm}^{-2}\,\text{s}^{-1}$,

he assumes bunches of 2.5×10^9 particles at a rate of $\gtrsim 1$ kHz and a disruption factor of 5. The bunches are to be focused to $\lesssim 10^{-2}\,\mu$m at the interaction point, requiring an emittance of order 10^{-12} cm-rad (assuming final $\beta \cong 1$ cm). Taking this emittance requirement and the plasma and wave parameters as $n_0 = 10^{16}\,\mathrm{cm}^{-3}$, $w \cong c/\omega_p = 50\,\mu$m, $eE_0/m\omega_p c \cong n_1/n_0 = 0.5$ (~ 5 GeV/m), and $\sin k_p\zeta_0 \lesssim 0.2$,[20] we find from Eq. (27) that a must be less than $0.2\,\mu$m ($k_p a < 0.004$). Although it is not clear how one could load such a large number of particles in such a narrow beam, the physics limitation suggested by Eq. (19′) is of order $N_0 \cong 0.6 \times 10^9$. This is within a factor of four of the number specified by Richter.

The focusing force produced by waves excited by square transverse beam profiles is less than the focusing force from waves excited by parabolic beam profiles.[21] From Eqs. (14) and (25), the focusing field resulting from a square driving-beam profile is $W_\perp = [-k_p^2 w K_1(k_p w) E_0 r \sin k_p\zeta]/[2(1 - k_p w K_1(k_p w)]$ (for $k_p r \ll 1$), and the inequality corresponding to Eq. (27) is

$$a \leq \sqrt{\varepsilon}\left\{\frac{2\gamma mc^2[1 - k_p w K_1(k_p w)]}{k_p^2 w K_1(k_p w) E_0 \sin k_p\zeta_0}\right\}^{1/4}.$$

Since K_1 decreases exponentially with $k_p w$, this inequality is easily satisfied for moderately wide waves. For our previous example, the inequality is satisfied for $a \cong w \gtrsim 0.3$ cm ($k_p w \approx 70$).

For dense accelerated beams, the wave field is not the only focusing force. In addition, there is a contribution to the betatron focusing force due to the transverse wake field of the beam itself [Eqs. (12) and (14)]. This force is zero at the head of the bunch and increases toward the tail, while the wave's focusing force ($\propto \sin\phi$) increases toward the head.

The maximum self-focusing force is of order[8] $2\pi ne^2 r \sin k_p(\zeta - \zeta_0)$, where n is the smaller of the beam density or plasma density. This force is dominant (for parabolic wave profiles) when

$$\frac{4\pi en}{k_p E_0}\frac{\sin k_p(\zeta - \zeta_0)}{\sin k_p\zeta_0}\left(\frac{k_p w}{2}\right)^2 > 1,$$

as in the case of dense, narrow beams in wide waves. For dense, narrow beams in waves c/ω_p wide, the wave focusing and self-focusing are of the same order, so the correction to Eq. (27) is only a factor of order $2^{1/4}$.

For waves and beams of equal width, shaped as in Section 3, it can be shown that the total focusing force never exceeds the focusing force of the wave at the head of the bunch.

4.2. *Efficiency*

In the previous example, the requirement of low emittance restricted the beam cross section to only 2×10^{-5} of the wave cross section. Fortunately, the efficiency depends on the overlap of the beam and wave *fields* and not the actual beam size.

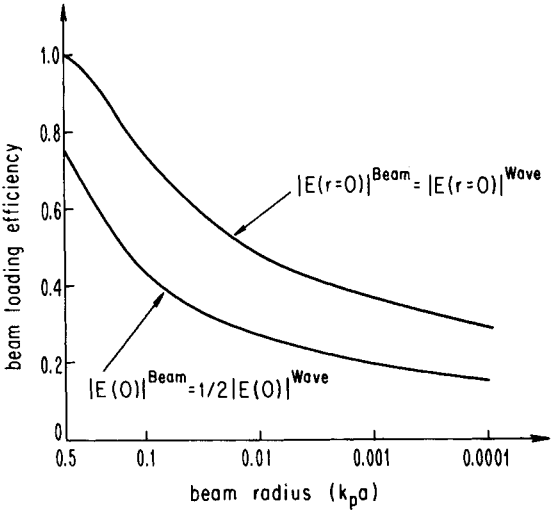

FIGURE 9 The beam-loading efficiency vs beam radius in a wave of diameter c/ω_p. The upper curve corresponds to an ultrashort beam with $N = N_0$ electrons [see Eq. (19′)]; the lower curve corresponds to a short beam with $N_0/2$ electrons or a shaped beam [Eq. (22′)] with $3N_0/4$ ecectrons.

Denoting the longitudinal field as E_0 and the wake field produced behind the beam as E_b, the efficiency is

$$\eta_b = 1 - \frac{\int_0^\infty [E_0(r) - E_b(r)]^2 r\, dr}{\int_0^\infty E_0^2(r) r\, dr}, \tag{28}$$

where the radial dependences are given by Eq. (25) with the appropriate values of a for each case. In Fig. 9, this efficiency is plotted as a function of beam radius for a wave of diameter c/ω_p (i.e., a wake field produced by a driving beam of radius 0.5 c/ω_p). The top curve assumes that $E_b(0) = E_0(0)$ (corresponding to 100% efficiency in one dimension), so that the fields behind the beam exactly cancel on axis. The lower curve corresponds to $E_b(0) = \frac{1}{2}E_0(0)$, as would be the case for beam loading according to Eq. (22′) with $\cos k_p\zeta_0 = \frac{1}{2}$. Applying the lower curve to our previous example ($k_p a \cong 0.004$), we predict the acceleration of $N = (\sin^2 k_p\zeta_0/2\cos k_p\zeta_0)N_0' \cong 0.3 \times 10^9$ electrons with 20% beam-loading efficiency. Of course, the overall efficiency of the accelerator is given by the product of this times the efficiency of the free energy source times the efficiency from source to plasma waves ($> 80\%$ in 1-D computer simulations we have performed previously).

4.3. Energy Spread

Assuming that the beam can be properly shaped [Eq. (22′)] so that the energy spread is made negligible for particles on axis, we now consider the contribution to energy spread due to the transverse variations of the longitudinal fields.

For light beam loading ($N \ll N_0'$), energy spread arises because the particles off axis feel a reduced wave field. This contributes a fractional energy spread of order

$$\frac{\Delta E}{E} \lesssim 1 - \frac{E_0(a)}{E_0(0)} \cong \frac{a^2}{w^2}, \tag{29}$$

for beams of radius a and waves of radius w. This is very small ($\sim 10^{-5}$) for the narrow beam we considered in our example.

A more significant contribution to the energy spread arises for dense, narrow beams due to the variation of the beam wake field across the beam itself. If the beam is narrower than the wave and shaped so that the total field is uniform on axis (within the beam), then off axis the total field is nonuniform, because the beam wake amplitude falls off more quickly than the wave amplitude. This gives rise to an energy spread

$$\frac{\Delta E}{E} \lesssim \frac{1 - \cos k_p \zeta_0}{\cos k_p \zeta_0} \left[1 - \frac{R_a(a)}{R_a(0)}\right], \tag{30}$$

where $R_a(r)$ is given by Eq. (25) and $k_p\zeta_0$ by Eqs. (22). For $k_p a$ much less than both unity and $k_p w$, the factor $(1 - R_a(a)/R_a(0))$ is approximately $-[0.154 + 2 \ln (k_p a/2)]^{-1}$. For our previous example of $k_p a = 0.004$ and $\cos k_p \zeta_0 = \frac{1}{2}$, this gives an energy spread of 8%.

5. SUMMARY

In summary, we have found the total number of particles that can be accelerated in a relativistic plasma wave. For ultrashort beams, the maximum particle number is

$$N_0 \cong 5 \times 10^5 \sqrt{n_0}\, A_{\text{eff}} \frac{n_1}{n_0}, \tag{19'}$$

where A_{eff} is the effective area of the beam [Eq. (19a')] and n_1/n_0 is the normalized wave amplitude (<1). For ultrashort unshaped bunches, the energy spread increases with the number of particles as N/N_0 [Eq. (20)] while the maximum efficiency scales as $N/N_0(2 - N/N_0)$ [Eq. (21)].

By employing specialized bunch shaping [Eqs. (22) and (22')], this energy spread can be eliminated, leaving only contributions due to phase slippage [Eq. (24)], shaping errors, and transverse field variation [Eq. (29) and (30)]. The maximum number of particles in the shaped bunch is $N_0 \sin^2 k_p\zeta_0/2 \cos k_p\zeta_0$. [Eq. (22d')], giving rise to a maximum efficiency of $\sin^2 k_p\zeta_0$ [Eq. (22e)], and gradient $E_0 \cos k_p\zeta_0$ [Eq. (22c)]. Emittance requirements may restrict the radius of the accelerated beam [Eq. (27)]. To meet this requirement while keeping the efficiency from becoming very low, we consider waves of width c/ω_p and narrow beams. In this case, $k_p a$ may be $\ll 1$ and A_{eff} becomes of order c^2/ω_p^2. The efficiency that results for mismatched beam and wave cross sections is illustrated for two cases in Fig. 9.

Based on these results, a nonoptimized set of parameters has been calculated that suggests a very low emittance beam of 3×10^8 electrons or positrons could be accelerated with greater than 20% beam-loading efficiency with a total energy spread as small as 8% (for negligible phase slippage). Optimization may improve these figures. The overall efficiency of the accelerator depends also on the efficiency of the free energy source and the efficiency of converting the source energy to plasma waves ($\gtrsim$80% in previous 1-D simulations).

The analytic results are consistent with 1-D simulations. Longer runs which follow the beam to more realistic energies, as well as 2-D simulations, are required. These are necessary to take into account simultaneously the effects of self-focusing, bunch distortion, and phase slippage.

ACKNOWLEDGMENT

We wish to thank P. Wilson, S. Van der Meer, and R. Ruth for suggestions that led to this work. This work was supported by USDOE P.A. DE-AS03-83ER40120, NSF PHY 84-20958, and LLNL 6223205.

REFERENCES

1. C. Joshi, W. B. Mori, T. Katsouleas, J. M. Dawson, J. M. Kindel, and D. W. Forslund, *Nature* **311,** 525 (1984).
2. T. Katsouleas *et al.*, in C. Joshi and T. Katsouleas, Eds., *Laser Acceleration of Particles, AIP Conf. Proc.* **130** (1985).
3. P. Chen, R. W. Huff, and J. M. Dawson, *Bull. Am. Phys. Soc.* **29,** 1355 (1984); P. Chen, J. M. Dawson, R. W. Huff, and T. Katsouleas, *Phys. Rev. Lett.* **54,** 693 (1985); P. Chen and J. M. Dawson, in C. Joshi and T. Katsouleas, Eds., Op. Sit.
4. T. Tajima and J. M. Dawson, *Phys. Rev. Lett.* **43,** 267 (1979); T. Katsouleas and J. M. Dawson, *Phys. Rev. Lett.* **51,** 392 (1983).
5. R. Ruth, A. Chao, P. Morton, and P. Wilson, *Particle Accelerators* **17,** 171 (1985).
6. K. L. F. Bane, P. Chen, and P. B. Wilson, *IEEE Trans. Nucl. Sci.* **NS-32,** 3524 (1985); P. Chen, J. J. Su, J. M. Dawson, K. L. F. Bane, and P. B. Wilson, *Phys. Rev. Lett.* **56,** 1252 (1986); T. Katsouleas, *Phys. Rev. A* **33,** 2056 (1986).
7. S. Van der Meer, CLIC Note No. 3, CERN/PS/85-65 (AA) (1985).
8. P. Chen, SLAC report SLAC-PUB-3823 (1985); also *Particle Accelerators* **20,** 171 (1985).
9. This was pointed out to us by J. Schwinger.
10. W. Panofsky and W. Wenzel, *Rev. Sci. Instrum.* **27,** 967 (1956).
11. J. Lawson, J. Allen, R. Bingham, T. Butterworth, F. Close, R. Evans, G. Rees, and R. Ruth, Rutherford Appleton Laboratory report RL-83057 (1983); R. Fedele, U. de Angelis, and T. Katsouleas, *Phys. Rev. A* **33,** 4412 (1986).
12. P. B. Wilson, Proc. Summer School on High Energy Particle Accelerators, Fermilab, 1981, SLAC report SLAC-PUB-2884 (1982).
13. K. Bane, private communication.
14. J. D. Jackson, *Classical Electrodynamics* (John Wiley & Sons, New York, 1975), 2nd ed., p. 118.
15. I. Gradshteyn and I. Ryzhik, *Tables of Integrals, Series, and Products* (Academic Press, New York, 1965), 4th ed., p. 683.
16. R. Evans in C. Joshi and T. Katsouleas, Eds., op. sit.; that the beam density would become greater than the plasma density for the parameters of Ref. 19 was pointed out by J. Lawson at the conference of Ref. 2.

17. D. Forslund, J. Kindel, W. B. Mori, C. Joshi and J. M. Dawson, *Phys. Rev. Lett.* **54,** 558 (1985); G. Schmidt, private communication; P. Sprangle and C. M. Tang in C. Joshi and T. Katsouleas, Eds., op. cit.
18. B. Zotter, LEP internal report (1985).
19. B. Richter in C. Joshi and T. Katsouleas, Eds., op. cit.
20. R. Ruth *et al.,* in Ref. 5, limit sin ϕ rather than a to meet the emittance requirement.
21. R. D. Ruth and P. Chen, Proc. of 13th SLAC Summer Institute on Particle Physics, July 1985, SLAC report SLAC-PUB-3906 (1985).